Texture-Induced Anisotropy in an Inconel 718 Alloy Deposited Using Electron Beam Freeform Fabrication

W Tayon[1], R Shenoy[2], R Bird[1], R Hafley[1] and M Redding[3]
[1] NASA Langley Research Center, Hampton, VA, USA
[2] Northrop Grumman Technical Services, Hampton, VA, USA
[3]Univerity of Virginia, Charlottesville, VA, USA
E-mail: wesley.a.tayon@nasa.gov

Abstract. A test block of Inconel (IN) 718 was fabricated using electron beam freeform fabrication (EBF^3) to examine how the EBF^3 deposition process affects the microstructure, crystallographic texture, and mechanical properties of IN 718. Tests revealed significant anisotropy in the elastic modulus for the as-deposited IN 718. Subsequent tests were conducted on specimens subjected to a heat treatment designed to decrease the level of anisotropy. Electron backscatter diffraction (EBSD) was used to characterize crystallographic texture in the as-deposited and heat treated conditions. The anisotropy in the as-deposited condition was strongly affected by texture as evidenced by its dependence on orientation relative to the deposition direction. Heat treatment resulted in a significant improvement in modulus of the EBF^3 product to a level nearly equivalent to that for wrought IN 718 with reduced anisotropy; reduction in texture through recrystallization; and production of a more homogeneous microstructure.

1. Introduction

Electron beam freeform fabrication (EBF^3) is a near-net-shape additive manufacturing technique for fabricating large-scale metal components that is currently being developed at NASA Langley Research Center for aerospace applications [1, 2]. Use of the EBF^3 process for fabrication of superalloy Inconel (IN) 718 components for high-temperature structural applications is being actively investigated. IN 718 is weldable [3], making it a viable candidate material for the EBF^3 process. Previous work [4] showed the EBF^3-deposited IN 718 material has good strength in the direction of the deposition; higher tensile and yield strengths than those obtained in conventional IN 718 castings, but lower than those for conventional cold-rolled sheets; and significantly lower Young's modulus (E) compared to conventionally-processed wrought or cast products. In a pure nickel single crystal, E varies strongly with crystal direction (Table 1), which may explain the lower E in the deposition direction. The objective of this study is to investigate the impact of texture on the E anisotropy in the EBF^3 product.

Table 1. Elastic modulus (GPa) dependence on crystal direction for pure Ni [5].

$E_{<111>}$	$E_{<110>}$	$E_{<100>}$
296	220	124

2. Experimental Procedures

Inconel 718 wire feedstock was deposited onto an IN 718 base plate using the EBF^3 process. The details of the EBF^3 process as relevant to the fabrication of this test block are provided in reference [4]. The base plate (12.7 mm thick) and feed wire (1.14 mm diameter) had a nominal composition (in weight percent) as follows: Ni - 19 Cr - 18 Fe - 5.1 (Nb + Ta) - 3 Mo - 0.9 Ti - 0.5 Al [3]. Room temperature precision modulus tests were conducted according to ASTM specification E111 [6] on specimens machined from the EBF^3 test block in each of the orientations of interest (L, T, 45°) labeled in Figure 1.

One set of specimens was kept in the as-deposited (AD) condition while a second set was heat treated using the following parameters: anneal at 1464 K for 4 hours then air cool to room temperature, followed by an age at 991 K for 8 hours then furnace cool to 894 K and hold for 8 hours, and finally air cool to room temperature. The goal of this heat treatment was to dissolve the undesirable, brittle Laves phase that forms during solidification and to minimize solute segregations in the dendritic microstructure [3]. In this study, it was employed to reduce the anisotropy observed in the AD condition via a modified grain structure and texture. Four specimens in each condition and orientation were tested.

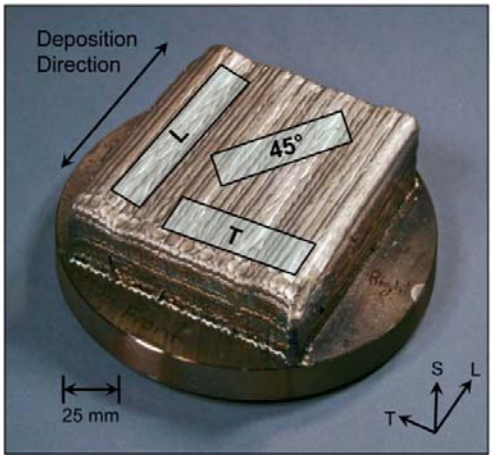

Figure 1. The IN 718 EBF3 block showing tensile specimen orientations L, T, and 45° in the L-T plane.

Electron backscatter diffraction (EBSD) was used to determine crystallographic orientation information on samples extracted from the AD and heat treated (HT) conditions. An estimated *E* based on EBSD data was also computed.

The *E* values for loading conditions parallel to the L, T, and 45° directions as computed from the EBSD data are reported as average values for the entire scanned EBSD area. These predictions were compared to mechanical test data to assess the agreement between the two and thence to confirm the extent of anisotropy present in the EBF[3] product. The EBSD analysis software computes an *E* value based on the Bishop-Hill average [7, 8] of elastic stiffness and the compliance tensors as described by Voigt [9] and Reuss [10]. Elastic constants were obtained from data from another Inconel alloy (IN 600) [11].

3. Results and Discussion

Experimentally measured (E_{prec}) and EBSD-computed (E_{EBSD}) *E* values for the AD and HT conditions are presented in Table 2. The published *E* values for typical as-cast and wrought products are also reported for comparison. Wrought property values were obtained from reference [12] for IN 718 following solution heat treatment and aging heat treatment in accordance with AMS 5596 [13]. As-cast properties were obtained from reference [14].

Table 2. *E* values (GPa) for IN 718 in the AD and HT conditions.

Test Orient.	As-Deposited		Heat Treated		Typical Cast	Typical Wrought
	E_{prec} (measured)	E_{EBSD} (computed)	E_{prec} (measured)	E_{EBSD} (computed)	Ref. [14]	Ref. [12]
L	138	156	174	170	199	198
T	194	210	192	184	199	206
45°	207	210	193	188	---	---

The measured *E* in the deposit was significantly lower (~30%) than published data for wrought IN 718 plate along the L direction (deposition direction). Along the T direction, the measured *E* in the AD condition was very close to the typical *E* value for wrought plate. *E* values along the 45° orientation were similar to those along T. In the HT condition, there was a significant increase in the measured *E* along the L direction relative to the AD condition. However, the improved E through heat treatment was still measurably lower relative to the wrought plate (~15% lower). In contrast, for both the T and the 45° orientations, the measured *E* values were equivalent to wrought plate. The low *E* values reported along L

strongly suggest a high concentration of grains with a <100> direction oriented parallel to the deposition direction. There was good agreement between the measured and EBSD-computed *E* values in both the AD and HT conditions, fully attesting to the contribution of texture to *E* anisotropy.

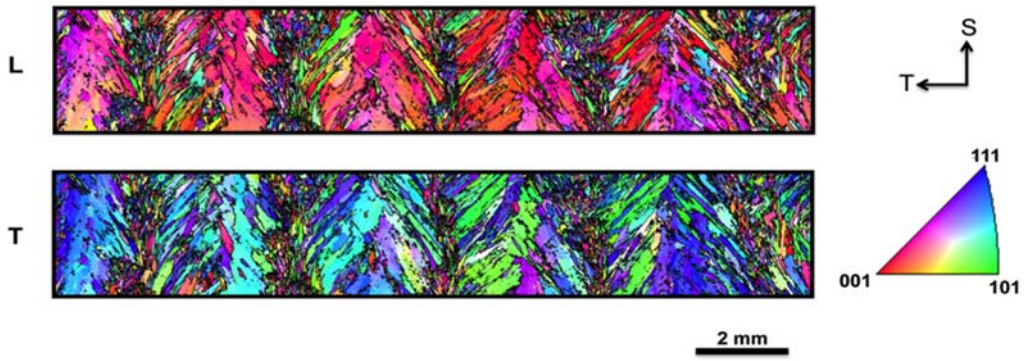

Figure 2. Inverse pole figure maps for IN 718 EBF³ block in the AD condition referenced to direction L (top) and direction T (bottom).

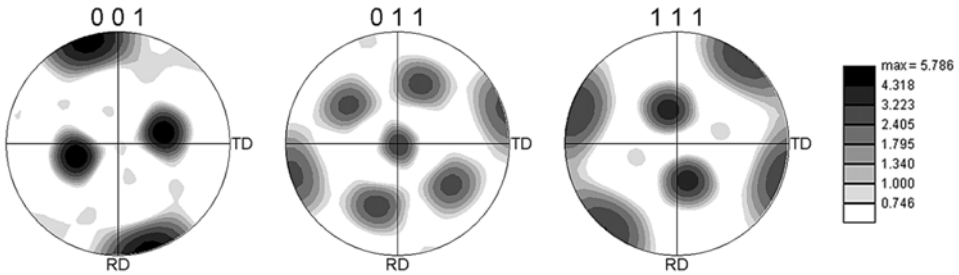

Figure 3. 001, 011, and 111 pole figures for the AD condition. The axes RD and TD correspond to the sample directions L and T, respectively.

The inverse pole figure maps presented in Figure 2 show that the microstructure within the EBF³ deposit was highly textured. The microstructure displays a range of strong texture components for L that are largely concentrated around <001> (top image). These directions are known to be low modulus orientations for Ni. In contrast, texture along T has <111> and <101> directions (bottom image), both known to be higher modulus orientations. Five distinct EBF³ deposited layers with a distinctly dendritic grain pattern can also be identified in these maps, with much smaller grains present at the inter-layer regions. Grain sizes ranged from approximately 1 mm down to several microns in diameter.

The EBSD-generated pole figures shown in Figure 3 revealed a strong Goss texture (slightly rotated about the S direction) and a preferential alignment of the [011] grains along the S direction of the EBF³ deposit. In addition, a strong [001] texture parallel to the L direction was also evident. Together, these data suggest the presence of a strong {011} <100>, Goss texture within the deposited layers.

An L-axis inverse pole figure map for the HT condition is shown in Figure 4. It clearly shows that heat treatment substantially recrystallizes the EBF³ deposited microstructure and appreciably decreases the extent of texture. Additionally, a more uniform grain size (~ 100 to 400 μm diameter) and a near equiaxed grain morphology were realized through this heat treatment compared to the AD condition.

The EBSD-generated pole figures shown in Figure 5 reveal a weak edge-on cube texture component present in the deposit. Such a texture is not uncommon in face centered cubic

metals subjected to static recrystallization [15]. This weaker texture reduces the extent of anisotropy in the HT condition compared to the AD condition.

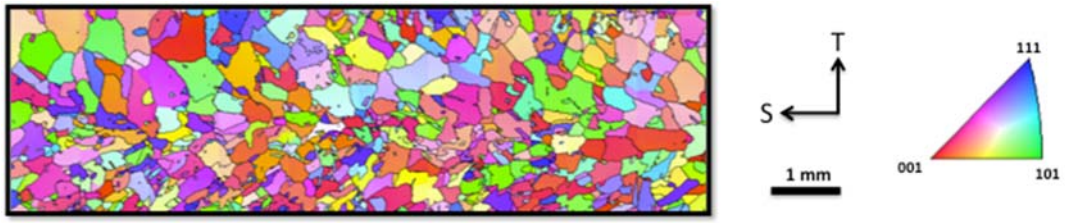

Figure 4. L-axis inverse pole figure map in IN 718 EBF³ block (HT condition).

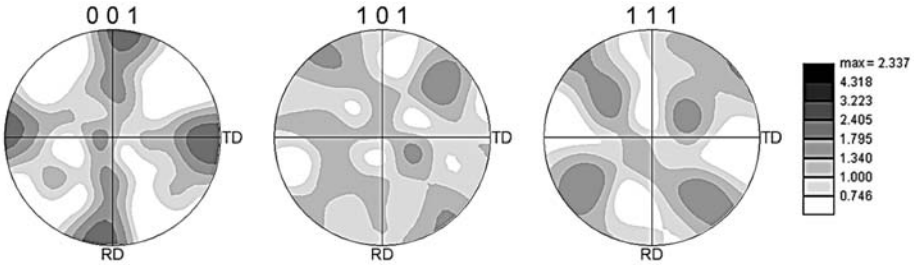

Figure 5. 001, 011, and 111 pole figures for IN 718 EBF³ block (HT condition).

4. Summary

Metallurgical characterization of an IN 718 block fabricated via the electron beam freeform fabrication (EBF³) process revealed a highly inhomogeneous and strongly textured microstructure. Elastic modulus values were strongly affected by texture as evidenced by their dependence on orientation relative to the deposition direction. Many grains were aligned with the low-modulus <100> direction in the deposition direction. Hence, the L direction was associated with the lowest values of *E*. Heat treatment significantly reduced the degree of texture, grain size heterogeneity, and anisotropy in the *E* values. Following heat treatment, *E* values were in better agreement with typical data for wrought plate.

5. References

[1] Taminger K and Hafley R 2006 NASA Technical Memorandum TM-2006-214284
[2] Taminger K and Hafley R 2003 *Proc. 3rd Annual Automotive Composites Conference* (Troy, MI)
[3] Brown W F and Setlak S (ed) 2005 *Aerospace Structural Metals Handbook* (West Lafayette, IN: CINDAS/USAF CRDA Handbook Operation, Purdue University)
[4] Bird R K and Hibberd J 2009 NASA Technical Memorandum TM-2009-215929
[5] Reed R 2006 *The Superalloys: Fundamentals and Applications* (Cambridge: Cambridge University Press)
[6] *Annual Book of ASTM Standards Vol. 3.01* 2010 (West Conshohocken, PA: American Society for Testing and Materials)
[7] Bunge H J et al 2000 *J Mech. Phys. Solids* **48** pp 29-66
[8] Bishop J F W and Hill R 1951 *Phil. Mag.* **42** pp 414-427
[9] Voigt W 1910 *Lehrbuch der Kristallphysik* (Berlin: Teubner)
[10] Reuss A 1926 *Zeitschrift für Angewandte Mathematik und Mechanik* **9**
[11] Dupond O et al 2011 *Journal of Physics: Conference Series* **269**
[12] Ruff P E 1986 Air Force Wright Aeronautical Laboratories Technical Report No. AFWAL-TR-85-4128
[13] *Aerospace Materials Specification AMS 5596K* 2007 (Warrendale, PA: SAE International)
[14] *Military Handbook - MIL-HDBK-5H: Metallic Materials and Elements for Aerospace Vehicle Structures* 1999 U.S. Department of Defense
[15] Doherty R D et al 1997 *Mater. Sci. Eng. A* **238** pp 219-274